Modeling of a Multizone Gas-Phase Polyethylene Reactor with a Cluster-Based Approach

H. Adli,[1] N. Mostoufi,[1] S. M. Ghafelebashi[2]

[1]*Process Design and Simulation Research Centre, Oil and Gas Processing Centre of Excellence, School of Chemical Engineering, College of Engineering, University of Tehran, P.O. Box 11155/4563, Tehran, Iran*
[2]*Polymer Research Group, Petrochemical Research and Technology Company, National Petrochemical Company, P.O. Box 14358/84711, Tehran, Iran*

Received 3 July 2010; accepted 24 November 2010
DOI 10.1002/app.33865
Published online 25 April 2011 in Wiley Online Library (wileyonlinelibrary.com).

ABSTRACT: A circulating fluidized reactor of polyethylene was modeled with the proper hydrodynamics for a riser and downer and combined with a kinetic model based on the moment equations. The hydrodynamic model was able to predict the profiles of the following parameters through the riser and downer: cluster velocity, bed porosity, concentration of potential active sites, active sites, gas-phase components, molecular weights, and reactor temperature. It was shown that one could control the monomer consumption and molecular weight, which are crucial in the reactor behavior and production properties, respectively, by setting different operating hydrodynamic conditions, such as the gas velocity in the riser and the solid circulation rate. © 2011 Wiley Periodicals, Inc. J Appl Polym Sci 122: 393–405, 2011

Key words: modeling; polyethylene (PE); reactive processing

INTRODUCTION

Polyethylene (PE) is the most widely used plastic today because of its low production cost, reduced environmental impact, and wide range of applications, such as in films, pipes, cables, adhesives, insulation, and electrical parts.[1] PE can be produced in three major commercial processes, solution, slurry (suspension), and gas phase. Gas-phase polymerization technology was recently developed for the manufacture of olefin polymers with high-activity transition-metal catalysts, such as Ziegler–Natta, chromium oxide, and supported metallocene catalysts. Gas-phase polymerization is used widely because of its low capital investment, low operational cost, lack of solvent separation, great heat-removal capability, use of different catalysts, and wide range of products.[2,3]

In recent years, many attempts have been made to develop applicable methods to improve polymer production and produce polymers with special properties. Some researchers have used conducting polymerization in two or more polymerization steps to produce PE.[4,5] In this method, polymers are prepared under different operating conditions in each step; therefore, the properties of the polymers are improved, and polymers with different molecular weights and compositions can be produced. However, polymers produced by multistep processes have low homogeneity. Covezzi and Mei[4] suggested a multizone circulating reactor (MZCR) for polymer production. In this method, polymerization occurs in two zones, and polymers circulate continuously; thus, polymers with more homogeneous structures can be produced. Fernandes and Lona[5,6] developed a mathematical model for the production of PE in such an MZCR. With the simplification of the kinetic model proposed by McAuley et al.[7] and with the assumption of steady-state and isothermal conditions, Fernandez and Lona[5] proposed a model for the simulation of typical behavior of an MZCR of the polymerization of ethylene. The effects of different parameters, such as the concentration of inert gas, catalyst flow rate, gas velocity, and porosity in the riser and downer, were investigated in their simulation. These simulation studies were also carried out in the case of the introduction of a gas barrier into the top of the downer.[6] Santos et al.[8] developed an isothermal, dynamic model for the MZCR, at particle and reactor levels, taking into account the particle population balance. This model is capable of predicting the polymer productivity, particle size distribution, and molecular weight and polydispersity of the polymer. In another study, Ghasem et al.[9,10] extended the model of Fernandez and Lona[5] to the dynamic model so that the transient behavior of the MZCR could be simulated. Moreover, the isothermal condition imposed by Santos et al.[8] and Fernandes and Lona[5] was employed in their study. The possible effects of the catalyst active site, potential active sites, reactor temperature, concentration of both ethylene and butane, catalyst feed rate, and molecular weight through the reactor length as a function of time were investigated. It is worth mentioning that in all of

Correspondence to: N. Mostoufi (mostoufi@ut.ac.ir).

these studies, it was assumed that the gas velocity, particle velocity, and porosity of the reactor were constant, both in the riser and downer. In other words, the effect of hydrodynamics on the performance of the reactor was neglected.

Hydrodynamic modeling of the riser and downer of a circulating fluidized bed can be easily found in the literature.[11–19] Most modeling efforts on these sections have been done according to the particle-based approach, by which it is assumed that the solids move as single particles.[11–14] In view of the fact that the existence of clusters in the riser and downer of fluidized beds is proved experimentally[19–23] and that the actual drag force exerted on the particles is higher than that for a single, isolated particle, it was proposed that the solids move in the riser and downer mainly in the form of clusters. Because the clusters are larger than single particles, the solid particles experience a higher drag force. Accordingly, Sabbaghan et al.[15] and Karimipour et al.[16] introduced the cluster-based approach (CBA) models for the riser and downer, respectively. They showed that the CBA provides a more realistic hydrodynamic description of the circulating fluidized bed compared to the particle-based approach.

In this article, a mathematical model is presented for the MZCR of PE with the CBA, by which the typical behavior of the reactor and polymer properties could be investigated. On the basis of this model, the porosity, particle velocity, monomer concentrations, and molecular weight were estimated, along the length of the reactor.

REACTOR MODELING

A simplified flow diagram of a circulating fluidized bed of PE production is shown in Figure 1. The reactor configuration provides polymerization in the gas phase in two polymerization zones made by two cylindrical, interconnected vertical legs, the riser and downer, in which the polymer is circulating continuously. The polymer particles move upward in the riser by means of a gas stream and downward in the downer by means of gravity. Polymer is transferred from the bottom of the downer through an L valve to the bottom of the riser. Nonreacted gases are compressed by a centrifugal compressor and recycled back to the bottom of the riser. Polymer is separated from the gas at the top of the riser by means of a cyclone, which discharges the solids to the top of the downer.

Assumptions

The assumptions made in developing the equations of the model are summarized as follows:

- The reactor operates at steady-state conditions.

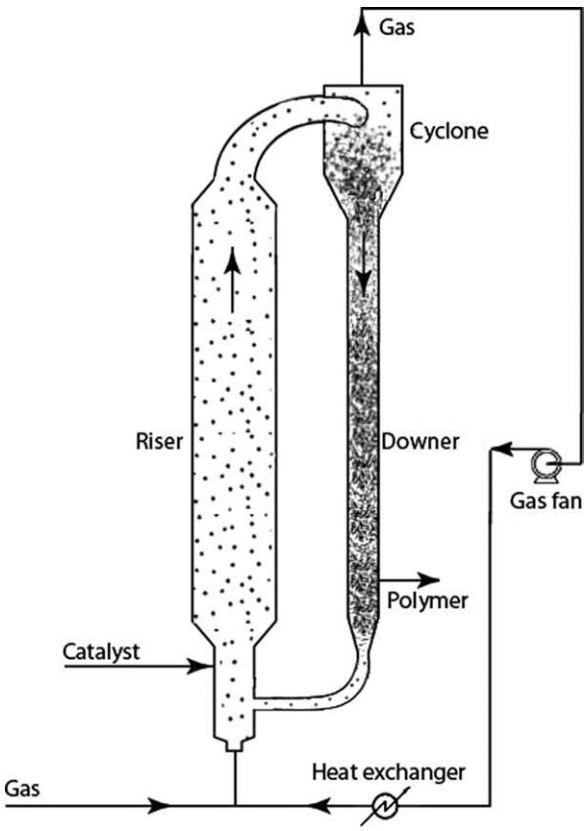

Figure 1 Schematic diagram of a circulating fluidized bed reactor.

- The flow pattern of the gas and polymer in both the riser and downer is plug, and the radial gradients are negligible.
- Catalyst is introduced continuously into the reactor as prepolymer.
- The catalyst is a single-site catalyst, and all catalytic sites are activated. For simplicity, it is considered that the catalyst does not suffer deactivation.
- Chain transfer to hydrogen is the sole chain-stopping event.
- Polymerization reactions occur only in the solid phase.
- The possible effect of heat generated in the activation, initiation, and chain transfer stages is neglected.

Model equations

The respective modeling equations for mass and energy balances are as follows:

$$\frac{dC_i}{dz} = -\frac{R_{pi}(1-\varepsilon)}{U_g} = \frac{R_{pi}(1-\varepsilon)}{U_0/\varepsilon} \tag{1}$$

$$\frac{dT}{dz} = \frac{\sum_{i=1}^{NC}(-\Delta H)R_{pi}(1-\varepsilon)}{\left[U_s C_p^* \rho_p (1-\varepsilon) + U_0 \varepsilon \sum_i \left(C_{pi} C_i\right)\right]} \tag{2}$$

where C_i is the monomer feed concentration (mol/L), z is the axial position (m), R_p is the production rate (kg/m^3 s), the subscript i indicates the monomer type number, ε is the axial average porosity, U_0 is the superficial gas velocity (m/s), T is the temperature (K), NC is the number of types of monomers, ΔH is the heat of reaction (kJ/mol), U_g is the gas velocity (m/s), U_s is the solid velocity (m/s), ρ_p is the particle density (kg/m^3), and C_p^* is the Polymer heat capacity (J/mol K). Equations for the concentration of potential active and active sites are given by

$$\frac{dR_0}{dz} = -\frac{kfR_0(1-\varepsilon)}{V_{cl}} \tag{3}$$

$$\frac{dR^*}{dz} = \frac{kfR_0(1-\varepsilon)}{V_{cl}} - \frac{\sum_{i=1}^{NC} ki_i C_i R^*(1-\varepsilon)}{V_{cl}} \tag{4}$$

where R_0 is the concentration of potential active sites, kf is the formation of active sites rate constant (s^{-1}), V_{cl} is the cluster velocity (m/s), R^* is the concentration of active sites, and ki_i is the rate constant for initiation by the monomer i (L mol^{-1} s^{-1}). In the model equations, the production rate of the polymer and concentrations of active site should be determined through a kinetic submodel. Also, the cluster velocity and porosity, either in the riser or in the downer, should be evaluated through the hydrodynamic submodel. The previous equations can be applied to both the riser and downer sections; the porosity of the bed and the cluster velocity in the equations must be changed to the porosity of the bed and the cluster velocity in either the riser or the downer.

Initial and boundary conditions

For solving the model equations, the initial conditions at the riser (i.e., gas concentration, polymer moments, and temperature) are the results of the downer section. Also, recirculation of catalyst and polymer from the downer to the riser are considered in the following equations:

$$R_0|_{z=0}^{r} = R_0|_{z=L}^{d} + q \tag{5}$$

$$\{Y_i, Q_i, T\}|_{z=0}^{r} = \{Y_i, Q_i, T\}|_{z=L}^{d} \tag{6}$$

where r is the riser, d is the downer, L is the length (m), q is the catalyst flow rate (g/s), Y_i is the moment i of the live polymer, and Q_i is the moment i of the dead polymer. The initial conditions of the downer (without a gas barrier) are gas concentration, polymer moments, and temperature, which should be obtained from the solution of the equations in the riser:

TABLE I
Elementary Reactions of the Ethylene Polymerization System

Type of reaction	Kinetic mechanism
Activation	$R_0 \xrightarrow{kf} R^*$
Initiation	$R^* + C_i \xrightarrow{ki_i} R_i(1)$
Propagation	$R_i(k) + C_j \xrightarrow{kp_{ij}} R_j(k+1)$
Monomer chain transfer	$R_i(k) + C_j \xrightarrow{kfm_{ij}} R_j(1) + Q(k)$
Hydrogen chain transfer	$R_i(k) + H_2 \xrightarrow{kfh_j} R_H(0) + Q(k)$

kfm_{ij}, transfer to monomer rate constant (L mol^{-1} s^{-1}); H_2, hydrogen feed concentration (mol/L); k, Chain length; $R_i(k)$, live polymer of length k with terminal monomer i; $R_j(k)$, live polymer of length k with terminal monomer j; $Q(k)$, dead polymer of length k; $R_H(0)$, active site produced by transfer to hydrogen; C_i, monomer i; C_j, monomer j.

$$\{Y_i, Q_i, T, C_i\}|_{z=0}^{d} = \{Y_i, Q_i, T, C_i\}|_{z=L}^{r} \tag{7}$$

The velocity of the solids in the downer is controlled by a valve at the bottom of this section, which transfers the solids to the riser. Accumulation of the solids would occur in neither the riser nor the downer. Therefore, the velocity of clusters at the top of the downer is calculated in a manner to keep the solid circulation rate the same in both sections. This clusters velocity can be calculated with Eq. (21).

Kinetics

A comprehensive mechanism was considered in this study to describe the copolymerization kinetics of ethylene and 1-butene over a Ziegler–Natta catalyst with a single catalyst site.[5] The kinetic mechanism comprises series and parallel elementary reactions, including site activation, propagation, and chain-transfer reactions. These reactions are listed in Table I. The kinetic parameters of ethylene polymerization for the Ziegler–Natta catalyst reported by McAuley et al.[7] were used in this study.

Characterization of the polymer properties was modeled with the method of moments. The moment equations are given in Table II. Application of the method of moments allows for the prediction of the physiochemical characteristics of the polymer, such as molecular weight, polydispersity, and other useful information of the system, such as polymer production rate and active site information. Once the moment equations were solved, the rate of reaction for each component, with the assumption that the monomers are mainly consumed through the propagation reactions, was obtained from[7]

$$Rp_i = \sum_{j=1}^{NC} kp_{ij} C_i Y_0 \phi_j \tag{8}$$

TABLE II
Moment Equations[5]

$$\frac{dY_0}{dz} = -\frac{\sum_{i=1}^{NC} ki_i C_i R^* (1-\varepsilon)}{V_{cl}}$$

$$\frac{dY_1}{dz} = \left[\sum_{j=1}^{NC} ki_i C_i R^* + \sum_{i=1}^{NC}\sum_{j=1}^{NC} kp_{ij} C_i Y_0 \varphi_j + \sum_{i=1}^{NC}\sum_{j=1}^{NC} kfm_{ij} C_i (Y_0 - Y_1)\varphi_j + \sum_{i=1}^{NC} kfh_j H_2 (Y_0 - Y_1)\varphi_j\right] \frac{(1-\varepsilon)}{V_{cl}}$$

$$\frac{dY_2}{dz} = \left[\sum_{j=1}^{NC} ki_i C_i R^* + \sum_{i=1}^{NC}\sum_{j=1}^{NC} kp_{ij} C_i (2Y_1 + Y_0)\varphi_j + \sum_{i=1}^{NC}\sum_{j=1}^{NC} kfm_{ij} C_i (Y_0 - Y_2)\varphi_j + \sum_{i=1}^{NC} kfh_j H_2 (Y_0 - Y_2)\varphi_j\right] \frac{(1-\varepsilon)}{V_{cl}}$$

$$\frac{dQ_k}{dz} = \left[\sum_{i=1}^{NC}\sum_{j=1}^{NC} kfm_{ij} C_i Y_k \varphi_j + \sum_{i=1}^{NC} kfh_j H_2 Y_k \varphi_j\right] \frac{(1-\varepsilon)}{V_{cl}}$$

kfh_i, transfer to hydrogen rate constant (L mol^{-1} s^{-1}); Y_k, moment k of the live polymer; Q_k, moment k of the dead polymer.

where kp_{ij} is the propagation rate constant for a polymer chain with terminal monomer i reacting with monomer j (L mol^{-1} s^{-1}), ϕ_j is the fraction of active sites with terminal monomer j. The number-average molecular weight (M_n; kg/kmol) and weight-average molecular weight (M_w; kg/kmol), respectively, could be calculated by the moment method with the following equations. In these equations, MW_m is the molecular weight of the monomer:

$$M_n = MW_m \frac{Q_1 + Y_1}{Q_0 + Y_0} \tag{9}$$

$$M_w = MW_m \frac{Q_2 + Y_2}{Q_1 + Y_1} \tag{10}$$

where Q_1 is the parameter in the correlation of Xu and Kato, Y_0 is the moment 0 of the live polymer, Y_1 is the moment 1 of the live polymer, Y_2 is the moment 2 of the live polymer, Q_0 is the moment 0 of the dead polymer, Q_1 is the moment 1 of the dead polymer, Q_2 is the moment 2 of the dead polymer. The polydispersity index (PDI) is the ratio of M_w to M_n:

$$PDI = \frac{M_w}{M_n} \tag{11}$$

Hydrodynamics

The flow pattern of gas and solids in fluidized beds are generally complex. As shown in Figure 1, the reactor of PE production considered in this study consisted of two distinct zones: the riser and the downer. In this study, the MZCR was modeled by the CBA technique through merging of the procedures developed by Sabbaghan et al.[15] and Karimipour et al.[16] for the riser and the downer, respectively.

Riser

As shown in Figure 2, the riser of the MZCR is divided into two distinct coexisting regions, that is, the lower density region, which is located right above the distributor, and the upper dilute region, which is located between the upper surface of the dense bed and the riser exit. The height of each region depends on the superficial gas velocity, solids circulation rate, and properties of the solids and fluid. The upper dilute region is between the upper surface of the dense bed and the reactor exit. This section itself is axially composed of three zones: the acceleration zone, where the solids are accelerated to a constant upward velocity; the fully developed zone above the acceleration zone, in which the flow characteristics are invariant with height; and the deceleration zone, which is located above the fully developed zone, where the solids are decelerated, depending on the exit geometry of the riser.[15] In this study, the smooth exit geometry was employed.

The lower dense zone is considered to operate at the turbulent regime of fluidization, the porosity of which can be estimated from[15]

$$\frac{\varepsilon_t - \varepsilon_{mf}}{1 - \varepsilon_{mf}} = 0.14 Re_p^{0.4} Ar^{-0.13} \tag{12}$$

where ε_t is the lower region porosity, ε_{mf} is the void fraction of the bed at minimum fluidization, Re_p is the particle Reynolds number [$d_p \rho_g V_p / \mu_g$, where d_p is the particle diameter (m), ρ_g is the gas density (kg/m^3), V_p is the particle velocity (m/s), and μ_g is the gas viscosity (Pa s)], and Ar is Archimedes number [$d_s^3 \rho_g (\rho_s - \rho_g) g / \mu^2$, where d_s is the diameter of fluidized species (m), ρ_s is the solid density (kg/m^3), g is the acceleration of gravity (m/s^2) and μ is the

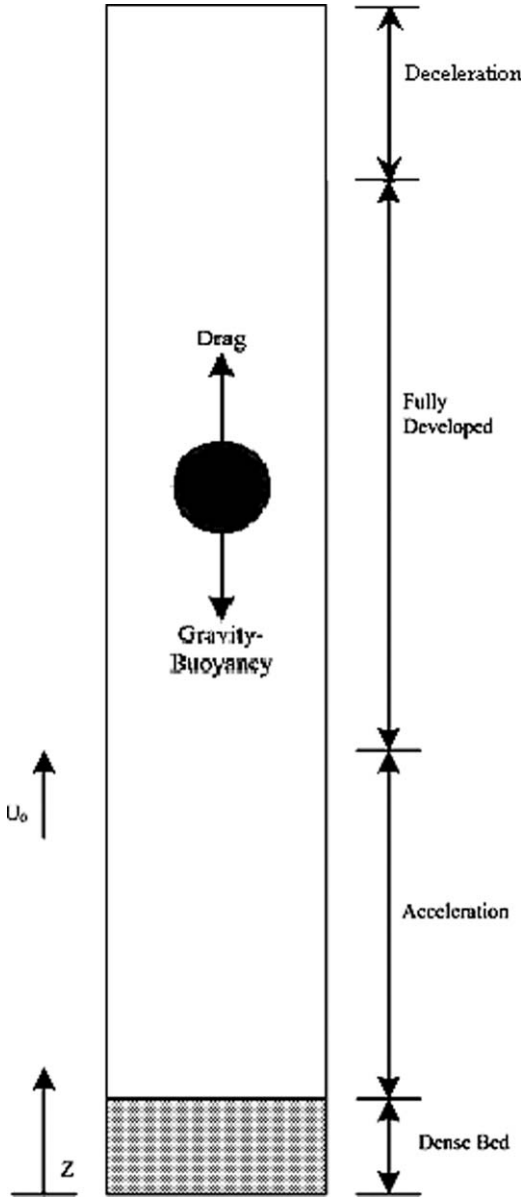

Figure 2 Different hydrodynamic zones of the riser.

gas viscosity (Pa s)]. The porosity of the beginning of the acceleration zone is considered to be the same as the porosity of the lower dense zone.

The cluster velocity in the acceleration and fully developed zones can be obtained by application of the one-dimensional force balance for the motion of the cluster:[15]

$$\frac{dV_{cl}}{dz} = \frac{3\rho_g C_D}{4d_{cl}\rho_{cl}} V_{cl} + \frac{1}{V_{cl}}\left(\frac{3\rho_g C_D}{4d_{cl}\rho_{cl}}\frac{U_0^2}{\varepsilon^2} + \frac{(\rho_g - \rho_{cl})g}{\rho_{cl}}\right) - \frac{3\rho_g C_D}{2d_{cl}\rho_{cl}}\frac{U_0}{\varepsilon} \quad (13)$$

where C_D is the effective drag coefficient, d_{cl} is the cluster diameter (m), and ρ_{cl} is the cluster density (kg/m^3). Equation (13) should be solved subject to the following initial condition:

$$V_{cl}|_{z=0} = \frac{G_s}{\rho_p(1-\varepsilon_t)} \quad (14)$$

where G_s is the solid circulation rate (kg/m^2 s), ε_t can be calculated from Eq. (13), and

$$\rho_{cl} = (1-\varepsilon_{cl})\rho_p + \varepsilon_{cl}\rho_g \quad (15)$$

where ε_{cl} is the Cluster porosity.

In this study, the porosity of clusters was assumed to be equal to the porosity at minimum fluidization conditions.

Once the cluster velocity was calculated, the void fraction in the riser can be determined from

$$\varepsilon = 1 - \frac{G_s}{\rho_p V_{cl}} \quad (16)$$

Other formulas required to solve the model are given in Table III.

Equation (13) can be applied to the deceleration zone of the riser. However, the boundary conditions for this zone are different than those of the acceleration zone. The porosity of the fully developed zone is taken as the initial condition for solving Eq. (13) in the deceleration zone:

$$\varepsilon|_{\text{start of deceleration}} = \varepsilon|_{\text{fully developed}} \quad (17)$$

However, the start of the deceleration zone is not known. Therefore, it should be obtained with the fact that the cluster velocity at the riser exit is equal to zero:

$$V_{cl}|_{\text{exit}} = 0 \quad (18)$$

Because the height of the deceleration zone is not known, it should be determined through a trial-and-error procedure, in which Eq. (13) is solved with the boundary condition in Eq. (17) for an estimated height of the deceleration zone. If the velocity is not zero at the end of integration, the height of the acceleration zone would be corrected. This procedure is repeated until a zero velocity equal to zero is obtained at the riser exit.

Downer

There are three distinct flow regions along the axial length of the downer, as shown in Figure 3. In the first region, the particle velocity is lower than the gas velocity. Hence, the particles are accelerated by both gravity and drag force. The action of both these forces in the same direction causes the particle velocity to increase sharply in this region. The second

TABLE III
Correlations Used in the Hydrodynamic Model

Parameter	Formula	Reference
Effective drag force coefficient	$C_D = fC_{D,0}$	24
	$C_{D,0} = \frac{24}{\mathrm{Re}_{cl}}(1 + 0.173\mathrm{Re}_{cl}^{0.657}) + \frac{0.413}{1 + 16300\mathrm{Re}_{cl}^{-1.09}}$	
	$f = \varepsilon^{-m}$	
	$m = 3.02\mathrm{Ar}^{0.22}\mathrm{Re}_t^{-0.33}\left(\frac{d_{cl}}{d_s}\right)^{0.40}$	
Cluster diameter	$\frac{d_{cl}}{d_p} = A\left(\frac{\rho_p}{\rho_{cl}}\right)$	25
	$A = \frac{(3333U_d g - M_2)(1-\varepsilon_{mf})(\rho_p - \rho_g)}{(Q_1 - 2M_2)\rho_p}$	
	$Q_1 = \frac{(\rho_p - \rho_g)g}{\rho_p}\left[U_0 + \frac{U_d\varepsilon_{mf}}{(1-\varepsilon_{mf})} + \frac{U_t\varepsilon_{mf}^{4.7}}{4}\right]$	
	$M_2 = \left(U_{mf} + \frac{U_d\varepsilon_{mf}}{(1-\varepsilon_{mf})}\right)g$	
Velocity of minimum fluidization	$\mathrm{Re}_{mf} = \left(33.7^2 + 0.0408Ar\right)^{0.5} - 33.7$	26
	$U_{mf} = \frac{\mathrm{Re}_{mf}\mu_g}{\rho_g d_p}$	

$C_{D,0}$, standard drag coefficient; f, drag force correction factor; $\mathrm{Re}_c i$, cluster Reynolds number ($d_{cl}\rho_g V_{cl}/\mu_g$); m, parameter in the correlation of Mostoufi and Chaouki; Re_t, particle terminal Reynolds number [$d_p\rho_g U_t/\mu_g$, where U_t is the terminal velocity (m/s)]; A, parameter in the correlation of Xu and Kato; U_d, solid superficial velocity (m/s); M_2, parameter in the correlation of Xu and Kato; U_{mf}, gas velocity at incipient of fluidization (m/s); Re_{mf}, particle Reynolds number at minimum fluidization velocity.

region begins when the particle velocity reaches the gas velocity. Drag and gravity forces in this region adversely act on the particle, and the acceleration rate becomes lower than that in the previous region. This situation is prolonged until the gravity and drag forces balance each other and the particle velocity becomes nearly constant in the next section. These three successive zones are named the first and second acceleration zones and the fully developed zone, respectively.

Karimipour et al.[16] adopted the CBA technique for modeling the downer and proposed the following force balance equation for one-dimensional motion of the clusters in the downer:

$$\frac{dV_{cl}}{dz} = \frac{3\rho_g C_D}{4d_{cl}\rho_{cl}V_{cl}}\left|\frac{U_0}{\varepsilon} - V_{cl}\right|\left(\frac{U_0}{\varepsilon} - V_{cl}\right) - \frac{g}{\rho_{cl}V_{cl}}(\rho_g - \rho_{cl}) \quad (19)$$

The porosity can be determined from the solids mass balance:

$$\varepsilon = 1 - \frac{G_s}{\rho_p V_{cl}} \quad (20)$$

At the top of downer, the particles are fluidized at the minimum fluidization condition before entering the downer.[27] Therefore, the solid mass balance can be employed to obtain the initial value of the cluster velocity, and Eq. (19) should be solved subject to the following initial condition:

$$V_{cl}|_{z=0} = \frac{G_s}{\rho_p(1-\varepsilon_{mf})} \quad (21)$$

RESULTS AND DISCUSSION

The results of MZCR modeling are in the form of a series of ordinary differential equations with initial

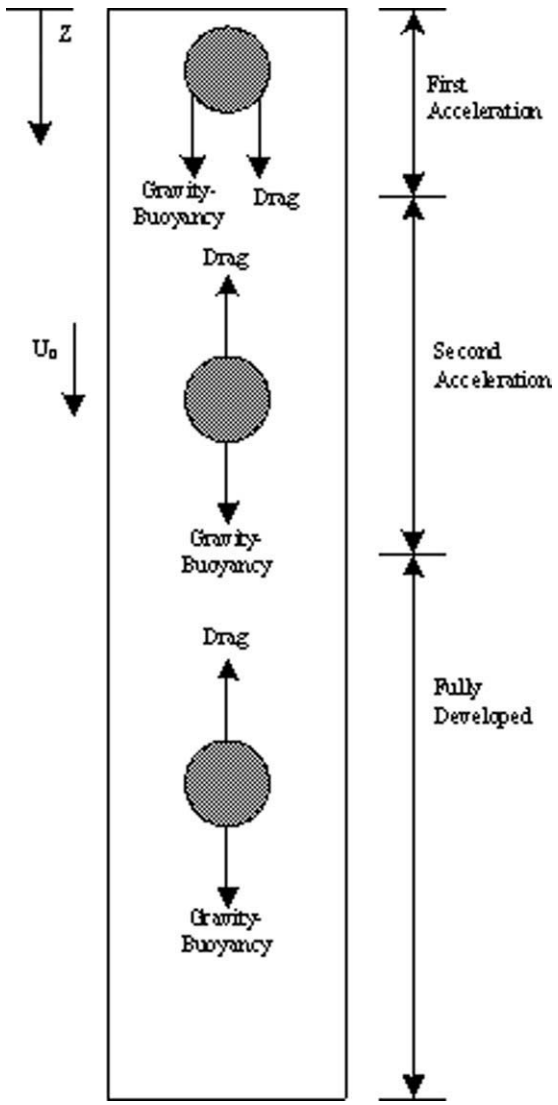

Figure 3 Different hydrodynamic zones of the downer.

TABLE IV
Operating Conditions and Input Parameters Used in the Simulations[2,6]

Parameter	Units	Value
Inlet temperature	°C	70
Pressure	atm	30
Particle diameter	μm	500
Riser		
Height	m	5
Diameter	m	0.3
Gas velocity	m/s	5
Ethylene concentration	kmol/m^3	0.320
1-Butene concentration	kmol/m^3	0.107
Hydrogen concentration	kmol/m^3	0.020
Nitrogen concentration	kmol/m^3	0.640
Catalyst makeup	g/s	0.2
Downer		
Height	m	3
Diameter	m	0.3
Gas velocity	m/s	0.4
Gas and polymer physical properties		
Gas density	kg/m^3	29
Gas viscosity	μPa s	11.6
Ethylene heat capacity	J/mol K	46
1-Butene heat capacity	J/mol K	100
Hydrogen heat capacity	J/mol K	27
Nitrogen heat capacity	J/mol K	28
Polymer density	kg/m^3	950
Polymer heat capacity	J/g K	1.839
Heat of reaction	kJ/mol	94.5

conditions that should be solved simultaneously. For solving the model equations, two steps are considered. In the first step, which is called the *cold model*, a circulating flow of the particles in the reactor is built up in a way that there is no reaction in the system. In this step, flow regimes within the riser and downer are created appropriately. In the second step, which is called the *hot model*, by feeding the catalyst into the reactor, one considers the polymerization reactions to occur, and the effects of different operating conditions on the performance of the reactor are investigated. It is worth noting that although the MZCR model developed in the previous section has not been validated against experimental polymerization data, the original models were separately validated against the experimental data.

Hydrodynamics of MZCR (cold model)

In all of the previous studies on the modeling of PE MZCRs in the literature,[5,8–10] it was assumed that there was a constant solid velocity and bed porosity along the riser and downer. However, we found during this study (shown in this section) that the effect of hydrodynamics was not negligible in the MZCR. In this section, the results of the solution of the hydrodynamic equations for the operating conditions shown in Table IV are presented. Solving the hydrodynamic model determined the axial profiles of cluster velocity and bed porosity in the riser and downer sections for the PE particles with the conditions presented in Table IV and three different solid circulation rates of 50, 250, and 450 kg m^{-2} s^{-1}.

Figure 4(a,b) demonstrates axial profiles of the cluster velocity and bed porosity for the riser, whereas Figure 5(a,b) shows these profiles for the downer. According to Figure 4(a), at the bottom of the riser, the gas accelerated polymer clusters and increased the solid velocity and porosity in the acceleration zone. Afterward, the cluster velocity and porosity reached a constant value in the fully developed zone. Finally, the cluster velocity and porosity decreased dramatically in the deceleration zone, and the solid velocity became zero at the exit. A comparison of Figures 4(a) and 5(a) revealed that with an increasing solid circulation rate, the cluster velocity

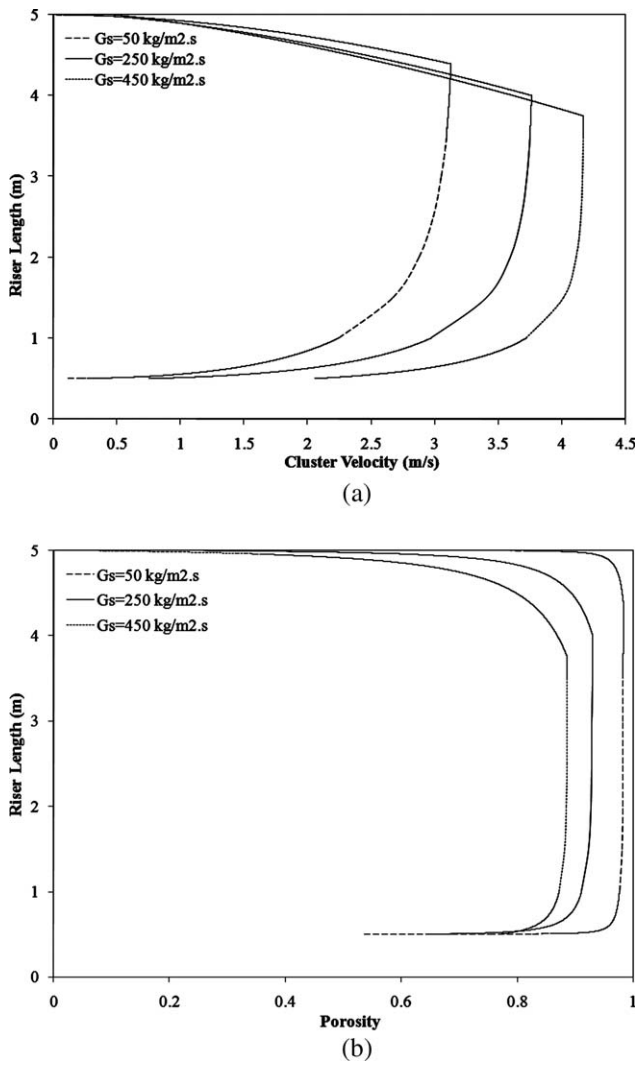

Figure 4 Model predictions of (a) the cluster velocity profile and (b) the bed porosity profile of PE particles in the riser at three solid circulation rates (50, 250, and 450 kg m^{-2} s^{-1}).

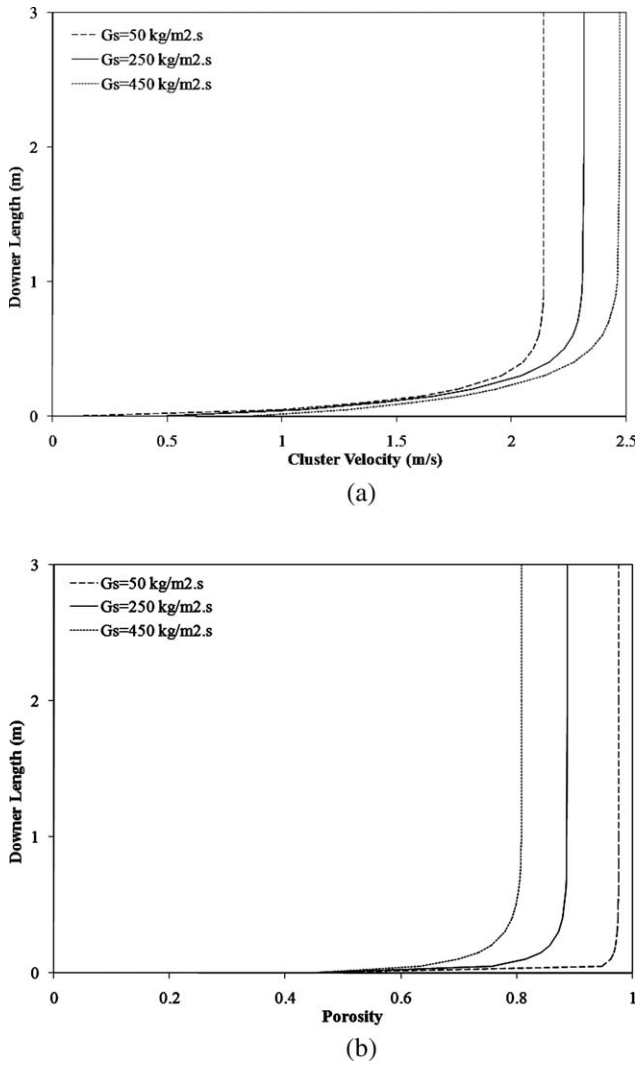

Figure 5 Model predictions of (a) the cluster velocity profile and (b) the bed porosity profile of PE particles in the downer at three solid circulation rates (50, 250, and 450 kg m^{-2} s^{-1}).

increased slightly for both the riser and the downer. Also, a comparison of Figures 4(b) and 5(b) revealed that with increasing solid circulation rate, the bed porosity value decreased for the riser and downer regions. Moreover, a comparison of Figures 4(a) and 4(b) revealed that increasing the solid circulation rate led to an increase in the height of both the deceleration and acceleration zones in the riser. Thus, a further increase in the solids circulation rate would result in a diminishment of the fully developed zone.

PE production in MZCR (hot model)

In this section, the behavior of MZCR, when we were feeding the catalyst and carrying out the polymerization reactions, was investigated by simultaneous solution of the differential equations of the kinetic and hydrodynamic models. These equations were solved by the assumption of steady-state and isothermal conditions.

Catalyst active site

When the fresh catalyst and cocatalyst were fed continuously to the reactor, they were quickly initiated to form active sites and live polymers. Figure 6 demonstrates the variation of concentration of catalyst potential active sites along the reactor at steady-state conditions. The number of potential active sites decreased because of polymerization reactions and, hence, depletion of the active sites. The decrease in the concentration of potential active sites was slower than that in the downer because of the shorter residence time and higher velocity of particles in the riser. The results reported by Ghasem et al.[9] are also shown in Figure 6, which demonstrates a similar trend for the variation of the concentration of catalyst potential active sites. However, a lower reduction of potential active sites was obtained by Ghasem et al.,[9] which was due to the assumption of constant particle velocity and bed porosity in both the riser and downer.

Figure 7 demonstrates the variation of the concentration of catalyst active sites along the reactor on the basis of the model developed in this work and the results reported by Ghasem et al.[9] This figure also shows that both models provided the same trend, and the differences between the two models were due to different values of the particle velocity and bed porosity in each model. Moreover, we observed that the number of active sites increased in the riser because of the continuous formation of active sites and slower reaction rate, whereas the consumption rate of active sites in the downer was higher than their formation rate because of the higher residence time in the riser. Therefore, the number of active sites decreased along the downer length.

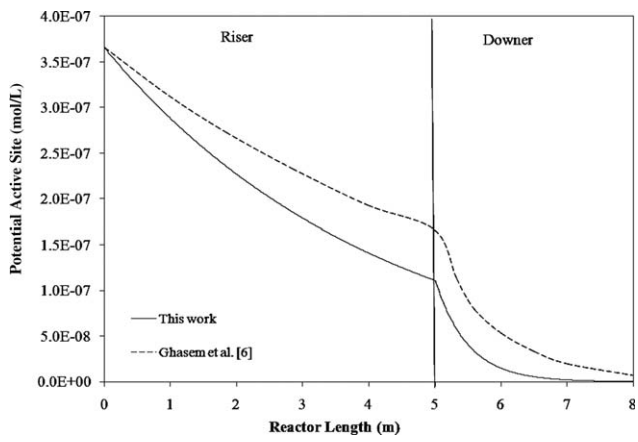

Figure 6 Concentrations of potential active sites in the riser and downer.

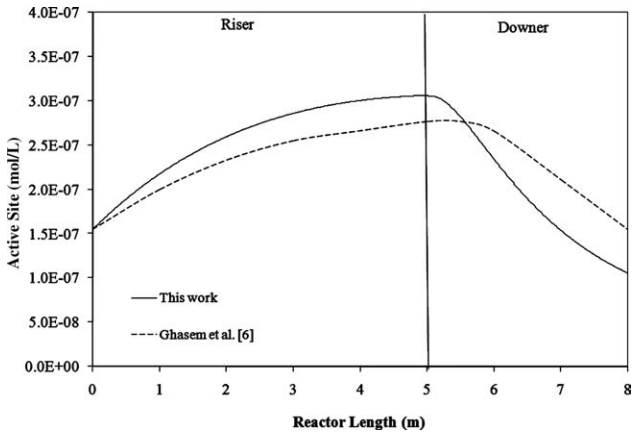

Figure 7 Concentrations of the active sites in the riser and downer.

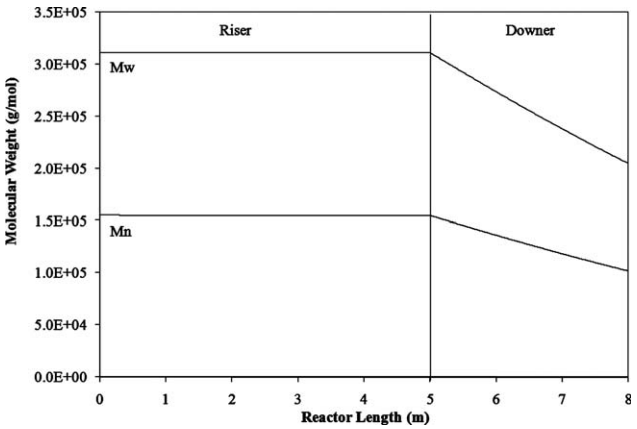

Figure 9 Instantaneous molecular weights in the riser and downer.

Monomer concentration profiles

The variation of the concentration of gas-phase monomers (ethylene and 1-butene) is shown in Figure 8. The concentration of these components was almost constant in the riser, whereas they decreased in the downer. In fact, the concentration of the monomers decreased slightly in the riser but cannot be seen in the scale of the figure. Decreases in the concentrations in both the riser and downer occurred because of their contribution to the copolymerization reactions. The consumption rate of ethylene was much higher than that of 1-butene because of the higher reactivity of ethylene compared to 1-butene. A low consumption of gas could be seen in the riser because of the short residence time of the particles in this section. On the other hand, the consumption of gas in the downer was relatively high because of the long residence time of the particles in this section.

Polymer properties

Molecular weight is a key factor that controls the physical and mechanical properties of polymeric materials. Figure 9 shows the instantaneous the profiles of the M_n and M_w values of the produced polymer in the reactor. The molecular weight of the polymer along the riser was almost constant because of the low polymerization reaction rate. In the downer, however, the polymer molecular weight decreased along the height because of reductions in the concentrations of both monomer and active sites.

A convenient parameter that characterizes the broadening of molecular weight distribution is PDI. Estimating this parameter is useful because polymer properties are not only dependent on the number of polymer chains but also on the dimensions and weight of each polymer chain. It was found that PDI approached 2 for the operating conditions shown in Table IV as the polymerization reaction proceeded. This index at steady-state conditions along the length of MZCR was almost constant and was the same in both the riser and the downer. This value was in agreement with that reported by Ghasem et al.[9]

Reactor temperature

Ethylene polymerization is exothermic. Thus, the temperature of the polymer tends to rise during the

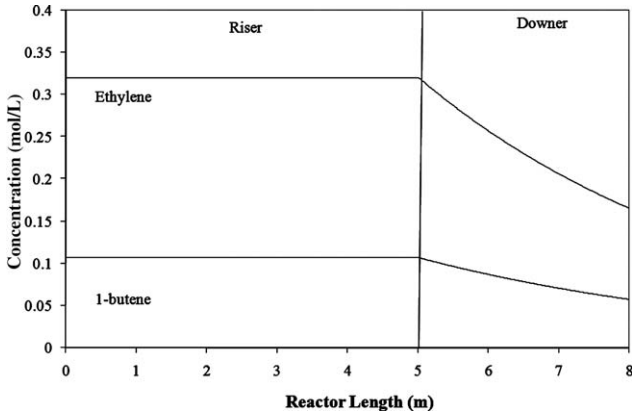

Figure 8 Concentrations of ethylene and 1-butene in the riser and downer.

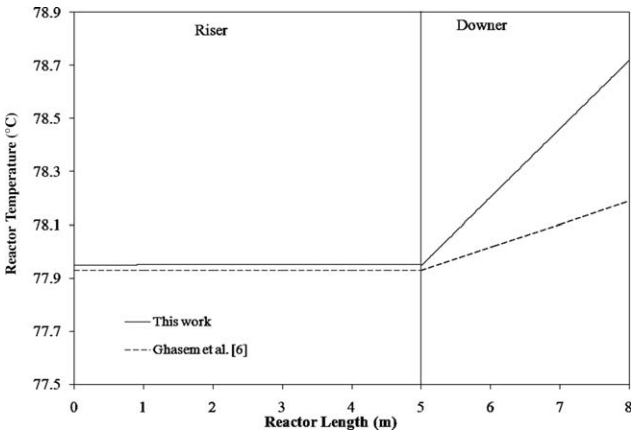

Figure 10 Temperature profile in the riser and downer.

progress of the reaction. If the temperature of the polymer particles exceeds its melting point, polymer particles could form agglomerates that might cause defluidization of the reactor. Figure 10 demonstrates the reactor temperature profile as a function of the reactor length at the steady-state condition, which we obtained by solving the energy balance equation. As can be observed in this figure, the temperature increase along the riser was negligible, whereas there was a slight increase in the temperature in the downer. This trend in the temperature of the reactor was also reported by Ghasem et al.[9] The negligible variation in temperature through the riser could be attributed to the low conversion of the monomer, which was associated with heat generation due to the reaction. In contrast, the temperature increase in the downer was mainly due to the higher conversion in this section.

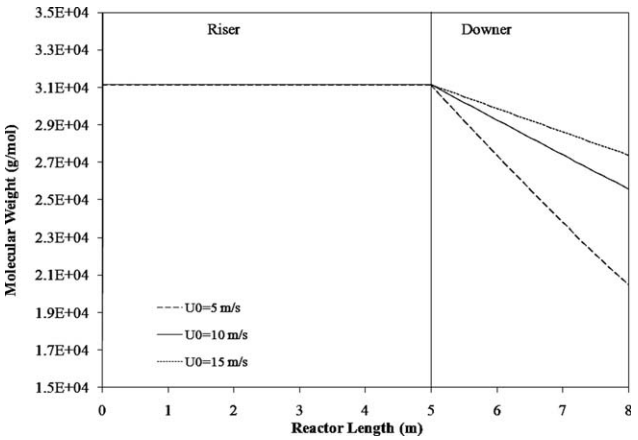

Figure 12 Instantaneous molecular weights in the riser and downer at three gas velocities in the riser (5, 10 and 15 m/s).

Effect of the gas velocity

The gas velocity affected the residence time of the reactants in the MZCR in both the riser and the downer. Figures 11 and 12 show the effects of the variation in gas velocity on the conversion of ethylene and the polymer properties. Gas velocity was varied between 5 and 15 m/s in the riser, whereas other operating conditions were kept constant. It can be seen in these figures that increasing the gas velocity did not have a significant effect on the profiles in the riser because the change in the riser was negligible because of the low conversion of the reactants in this section. However, increasing the gas velocity in the downer led to a lower conversion of monomer concentration in this region. A higher gas velocity in the riser increased the particle velocity in this section and, thus, transferred more particles to the downer. Therefore, to maintain the bed weight at steady state, the transfer of more particles to the riser was needed, which meant an increase in the velocity and a decrease in the residence time of the particles in the downer. The higher velocity resulted in lower gas consumption per pass in both sections. As a result, there would have been a lower rate of reduction of molecular weight of the polymer with the lower decrease in the gas concentration along the reactor, and the molecular weight would have tended to remain almost constant throughout the reactor. As a result, with increasing gas velocity in the riser because the monomer concentration remained at a higher level, the polymerization reaction rate and molecular weight increased through the reactor length.

Effect of the solid circulation rate

Variation of the solid circulation rate affected the concentration of active sites by changing the amount of particles in the reactor. Figures 13 and 14

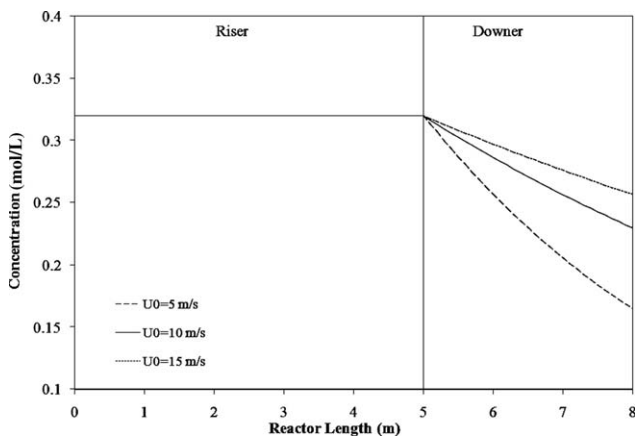

Figure 11 Concentrations of ethylene in the riser and downer at three gas velocities in the riser (5, 10, and 15 m/s).

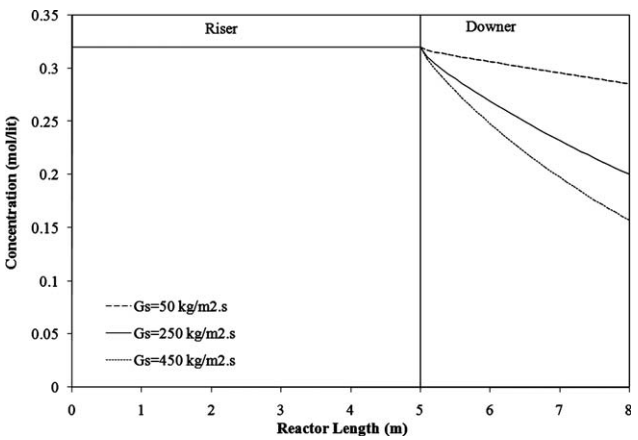

Figure 13 Concentrations of ethylene in the riser and downer at three solid circulation rates [50, 250, and 450 kg/(m^2 s)].

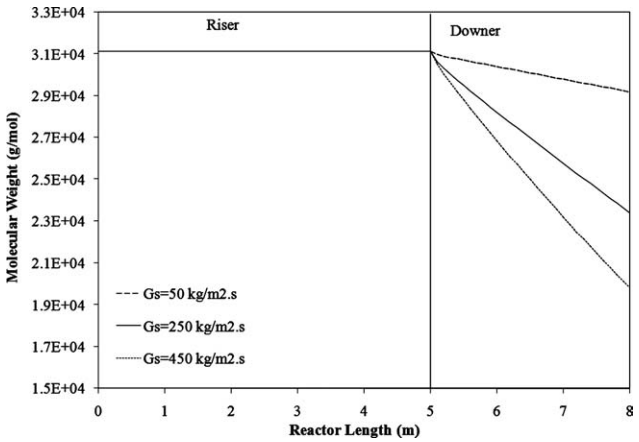

Figure 14 Instantaneous molecular weights in the riser and downer at three solid circulation rates [50, 250, and 450 kg/(m^2 s)].

illustrate the effect of the solid circulation rate on the concentration of ethylene and the molecular weight of the polymer in the reactor, respectively. Solid circulation rates of 50, 250, and 450 kg/(m^2 s) were simulated, whereas other operating conditions remained constant. According to these figures, an increase in the solid circulation rate led to a negligible increase in monomer consumption in the riser, although this increase in the solid circulation rate led to a much higher monomer consumption for the downer because of higher hold up of particles in this section. The effect of the increase in the solid circulation rate on the molecular weight in the downer was also significant, mainly because of the reduction in bed porosity and the increase in the solid-phase concentration. As a result, more active sites were available for the gas phase to contribute to the polymerization reaction. Consequently, a higher solid circulation rate would produce shorter polymers chains with lower molecular weights.

Effects of the ethylene and hydrogen concentrations

The effect of the variation of ethylene concentration on the polymer molecular weight through the reactor is presented in Figure 15. As can be seen in this figure, an increase in ethylene concentration from 0.32 to 0.52 mol/L increased the PE molecular weight because of the increase in the length of polymer chains.

The presence of hydrogen in the ethylene polymerization with a Ziegler–Natta catalyst reduced the polymer molecular weight because hydrogen acted as a chain-transfer agent and terminated polymerization reactions. The effect of the variation of hydrogen concentration on the PE molecular weight through the reactor is shown in Figure 16. According to this figure, an increase in hydrogen concentration from

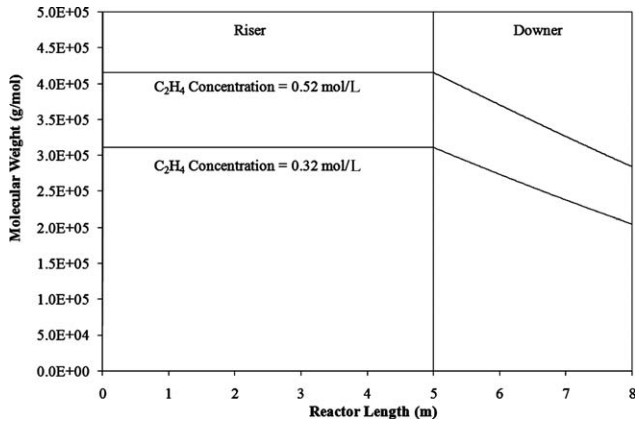

Figure 15 Instantaneous molecular weights in the riser and downer at ethylene concentrations of 0.32 and 0.52 mol/L.

0.02 to 0.2 mol/L led to a sharp reduction of polymer molecular weight through the reactor length.

CONCLUSIONS

A new comprehensive model was proposed to describe the behavior of a multizone circulating fluidized bed reactor of PE production with CBA. The model considers both the riser and downer sections. Plug flow of gas and solids through the riser and downer was assumed. The hydrodynamic model was based on the assumption that the solid phase moves as clusters rather than single, isolated particles. The kinetic model was based on the moment equations. The hydrodynamic and kinetic models were combined to develop a comprehensive model for gas-phase polymerization in MZCR. This model successfully predicted essential reactor parameters, such as monomer concentration profiles, M_n, M_w, and reactor temperature, along the reactor length. However, it can be proposed to include diffusion limited reactions in the future to obtain more precise results. Also, the effects of changes in the

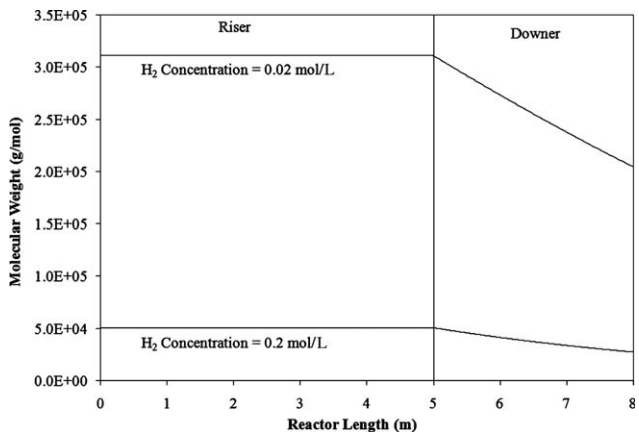

Figure 16 Instantaneous molecular weights in the riser and downer at hydrogen concentrations of 0.02 and 0.2 mol/L.

hydrodynamic parameters of the reactor behavior and the properties of polymers were discussed. It was observed that changes in reactor behavior and polymer characteristics due to polymerization reactions along the riser length were negligible. However, such changes led to reductions of monomer concentration and molecular weight of produced polymer chains in the downer. Moreover, increases in gas velocity in the riser and solid circulation rate decreased the reduction rate of monomer concentration and molecular weight of the produced polymer chains in the downer region. These changes did not affect obtained results in the riser.

NOMENCLATURE

A	parameter in the correlation of Xu and Kato
Ar	Archimedes number $[d_s^3\rho_g(\rho_s - \rho_g)g/\mu^2]$
C_D	effective drag coefficient
$C_{D,0}$	standard drag coefficient
C_i	monomer feed concentration (mol/L; $i = 1$ for ethylene and $i = 2$ for butene)
C^*_p	Polymer heat capacity (J/mol K)
C_j	monomer j
d	downer
d_{cl}	cluster diameter (m)
d_p	particle diameter (m)
d_s	diameter of fluidized species (m)
f	drag force correction factor
g	acceleration of gravity (m/s^2)
G_s	solid circulation rate (kg/m^2 s)
H_2	hydrogen feed concentration (mol/L)
k	chain length
kf	formation of active sites rate constant (s^{-1})
kfh_i	transfer to hydrogen rate constant (L mol^{-1} s^{-1})
kfm_{ij}	transfer to monomer rate constant (L mol^{-1} s^{-1})
ki_i	rate constant for initiation by the monomer i (L mol^{-1} s^{-1})
kp_{ij}	propagation rate constant for a polymer chain with terminal monomer i reacting with monomer j (L mol^{-1} s^{-1})
L	length (m)
m	parameter in the correlation of Mostoufi and Chaouki
M_2	parameter in the correlation of Xu and Kato
M_n	number-average molecular weight (kg/kmol)
M_w	weight-average molecular weight (kg/kmol)
MW_m	molecular weight of the monomer
NC	number of types of monomers
PDI	polydispersity index
q	catalyst flow rate (g/s)
Q_1	parameter in the correlation of Xu and Kato
Q_i	moment i of the dead polymer
Q_0	moment 0 of the dead polymer
Q_1	moment 1 of the dead polymer
Q_2	moment 2 of the dead polymer
Q_k	moment k of the dead polymer
$Q(k)$	dead polymer of length k
r	riser
R^*	concentration of active sites
R_0	concentration of potential active sites
Re_{cl}	cluster Reynolds number $(d_{cl}\rho_g V_{cl}/\mu_g)$
Re_{mf}	particle Reynolds number at minimum fluidization velocity
Re_p	particle Reynolds number $(d_p\rho_g V_p/\mu_g)$
Re_t	particle terminal Reynolds number $(d_p\rho_g U_t/\mu_g)$
$R_H(0)$	active site produced by transfer to hydrogen
$R_i(k)$	live polymer of length k with terminal monomer i
$R_j(k)$	live polymer of length k with terminal monomer j
R_p	production rate (kg/m^3 s)
T	temperature (K)
U_0	gas superficial velocity (m/s)
U_d	solid superficial velocity (m/s)
U_g	gas velocity (m/s)
U_{mf}	gas velocity at incipient of fluidization (m/s)
U_s	solid velocity (m/s)
U_t	terminal velocity (m/s)
V_{cl}	cluster velocity (m/s)
V_p	particle velocity (m/s)
Y_i	moment i of the live polymer
Y_0	moment 0 of the live polymer
Y_1	moment 1 of the live polymer
Y_2	moment 2 of the live polymer
Y_k	moment k of the live polymer
z	axial position (m)

Greek letters

ΔH	heat of reaction (kJ/mol)
ε	axial average porosity
ε_{cl}	Cluster porosity
ε_{mf}	void fraction of the bed at minimum fluidization
ε_t	lower region porosity
μ,μ_g	gas viscosity (Pa s)
ϕ_j	fraction of active sites with terminal monomer j
ρ_{cl}	cluster density (kg/m^3)
ρ_g	gas density (kg/m^3)
ρ_p	particle density (kg/m^3)
ρ_s	solid density (kg/m^3)

Subscript

i	monomer type number

References

1. Touloupides, V.; Kanellopoulos, V.; Pladis, P.; Kiparissides, C.; Mignon, D. Chem Eng Sci 2010, 65, 3208.
2. Rokkam, R. G.; Fox, R. O.; Muhle, M. E. Powder Technol 2010, 203, 109.
3. Dompazis, G.; Kanellopoulos, V.; Kiparissides, C. Macromol Mater Eng 2005, 290, 525.
4. Covezzi, M.; Mei, G. Chem Eng Sci 2001, 56, 4059.
5. Fernandes, F. A. N.; Lona, L. M. F. J Appl Polym Sci 2004, 93, 1042.
6. Fernandes, F. A. N.; Lona, L. M. F. J Appl Polym Sci 2004, 93, 1053.
7. McAuley, K. B.; Macgregor, J. F.; Hamielec, A. E. AIChE J 1990, 36, 837.
8. Santos, J. L.; Asua, J. M.; de la Cal, J. C. Ind Eng Chem Res 2005, 45, 3081.
9. Ghasem, N. M.; Ang, W. L.; Hussain, M. A. Chem Prod Process Model 2008, 3, Article 1.
10. Ghasem, N. M.; Ang, W. L.; Hussain, M. A. Korean J Chem Eng 2009, 26, 603.
11. Zhou, H.; Flamant, G.; Gauthier, D.; Lu, J. Int J Multiphase Flow 2002, 28, 1801.
12. Das, A. K.; Baudrez, E.; Marin, G. B.; Heynderickx, G. J. Ind Eng Chem Res 2003, 42, 2602.
13. Jian, H.; Ocone, R. Powder Technol 2003, 138, 73.
14. Li, S.; Lin, W.; Yao, J. Powder Technol 2004, 145, 73.
15. Sabbaghan, H.; Sotudeh-Gharebagh, R.; Mostoufi, N. Powder Technol 2004, 142, 129.
16. Karimipour, S.; Mostoufi, N.; Sotudeh-Gharebagh, R. Ind Eng Chem Res 2006, 45, 7204.
17. Hakimelahi, N.; Sotudeh-Gharebagh, R.; Mostoufi, N. Int J Chem Reactor Eng 2006, 4, Article 23.
18. Bolkan, Y.; Berruti, F.; Zhu, J.; Milne, B. Powder Technol 2003, 132, 85.
19. Huilin, L.; Qiaoqun, S.; Yurong, H.; Yongli, S.; Ding, J.; Xiang, L. Chem Eng Sci 2005, 60, 6757.
20. Liu, X.; Gaoa, S.; Li, J. Chem Eng J 2005, 105, 193.
21. Lu, X.; Li, S.; Du, L.; Yao, J.; Lin, W.; Li, H. Chem Eng J 2005, 112, 23.
22. Nova, S.; Krol, S.; de Lasa, H. Powder Technol 2004, 148, 172.
23. Pugsley, T. S.; Berruti, F. Powder Technol 1996, 89, 57.
24. Mostoufi, N.; Chaouki, J. Chem Eng Sci 1999, 54, 851.
25. Xu, G.; Kato, K. Chem Eng Sci 1999, 54, 1837.
26. Wen, C. Y.; Yu, Y. H. AIChE J 1966, 12, 610.
27. Johnston, P. M.; de Lasa, H. I.; Zhu, J. Chem Eng Sci 1999, 54, 2161.